



Published in final edited form as:

Cell Immunol. 2007 February ; 245(2): 80–90.

Maternal Microchimerism Leads to the Presence of Interleukin-2 in Interleukin-2 Knock Out Mice: Implications for the Role of Interleukin-2 in Thymic Function

Lucile E. Wrenshall^{*}, Elliot T. Stevens[†], Deandra R. Smith^{*}, and John D. Miller^{*}

^{*} *Division of Transplantation, University of Nebraska Medical Center, Omaha, NE 68198*

[†] *College of Veterinary Medicine, Kansas State University, Manhattan, KS 66506 (current address, E Stevens)*

Abstract

The role of interleukin-2 (IL-2) in thymic development is uncertain. Not surprisingly, IL-2 knockout (KO) mice have been used to address this question. However, as we report here, such mice are chimeric, containing both IL-2 KO cells and IL-2-expressing cells transferred *in utero* from their heterozygous mothers. These cells produce IL-2 in amounts detectable by conventional means, and their presence in lymphoid tissues confounds efforts to define the true IL-2 KO phenotype. To minimize the amount of IL-2 available to the thymus, we subjected recombinase activating gene – 1 KO mice to bone marrow transplantation using IL-2 KO donors, and then followed the reconstitution of the thymus. The thymuses of these mice became increasingly aberrant over time, including abnormalities in both stromal cells and thymocytes. These results demonstrate that IL-2 is critical to several aspects of thymic function, a finding previously obscured by the presence of IL-2 in IL-2 KO mice.

Keywords

interleukin 2; thymus; knock out; chimerism; murine

Introduction

Production of IL-2 is precisely regulated during development of the thymus [1–3], and deficiencies in either IL-2 or IL-2 receptor signaling result in severe lymphoproliferative and autoimmune disorders [4–6]. In light of these observations, one would expect IL-2 to have a significant influence on thymic development, yet the literature in this regard is unclear [5,7–9]. For example, Jenkinson et al. blocked IL-2 receptor signaling in fetal thymic organ cultures and found that both thymocyte proliferation and expression of the T cell receptor were inhibited [7]. However, in a similar system, Plum and De Smedt concluded that blockade of IL-2 receptor signaling has no effect on thymocyte development [9]. Subsequently, Schorle et al. reported that thymic cell populations were normal in IL-2 deficient mice [5], yet Kramer et al. found that the immunopathology evident in IL-2 deficient mice is thymus-dependent [10]. Finally,

Corresponding author: Dr. Lucile Wrenshall, University of Nebraska Medical Center, 983285 Nebraska Medical Center, Omaha, NE 68198-3285. Phone: 402-559-7871; fax: 402-559-3434; email: lwrenshall@unmc.edu. Address reprint requests to Dr. Wrenshall.

Publisher's Disclaimer: This is a PDF file of an unedited manuscript that has been accepted for publication. As a service to our customers we are providing this early version of the manuscript. The manuscript will undergo copyediting, typesetting, and review of the resulting proof before it is published in its final citable form. Please note that during the production process errors may be discovered which could affect the content, and all legal disclaimers that apply to the journal pertain.

studies examining a potential role for IL-2 in negative selection demonstrated a role for IL-2 in the thymic deletion of autoreactive CD4⁺ but not CD8⁺ thymocytes [8,11].

We questioned whether the apparently conflicting observations regarding the role of IL-2 in thymic function might be explained by the model systems used. Because IL-2 deficient mice are nearly always the offspring of heterozygous mothers [due to the poor health and shortened lifespan of IL-2 deficient females (5)], we reasoned that IL-2 KO mice born to heterozygous mothers might contain IL-2 or IL-2 producing cells that pass through the placenta. The presence of varying amounts of IL-2 in IL-2 KO mice could alter the phenotype of these mice. Because maternal transmission of cells is detectable in all offspring, when methods of sufficient sensitivity are used [12,13], we felt that the possibility of detecting IL-2 in IL-2 KO mice was strong enough to warrant further study.

Here we show that cells expressing IL-2 are present in the thymus and other lymphoid tissues of IL-2 KO mice. This chimerism complicates interpretations of the IL-2 KO phenotype and may be responsible, at least in part, for inconsistent results with respect to the impact of IL-2 on the thymus.

In light of these findings, we sought to assess thymic function in the absence or near absence of IL-2. To this end, we reconstituted recombinae activating gene – 1 (RAG-1) KO thymuses with either IL-2 wildtype (WT) or IL-2 KO bone marrow. We found that by 17 weeks post-transplantation, IL-2 was barely detectable in IL-2 KO→RAG-1 KO bone marrow chimeras. In addition, the morphology of the thymus and cell populations comprising the thymus were extremely abnormal as compared to RAG-1 KO mice reconstituted with IL-2 WT marrow. Our studies suggest that IL-2 plays an important role in thymocyte survival, differentiation, and maintenance of the thymic medulla.

Materials and Methods

Mice and bone marrow chimeras

BALB/c RAG-1 KO mice were purchased from the Jackson Laboratory (Bar Harbor, ME). DO11.10/IL-2 KO and DO11.10 mice on a BALB/c background were from our mouse colony at the University of Nebraska Medical Center. DO11.10 mice were originally obtained from Dr. M. Jenkins (University of Minnesota, Minneapolis, MN) and bred with BALB/c IL2^{+/-} males (The Jackson Laboratory, Bar Harbor, ME). Note that all of the IL-2 KO BALB/c mice used in the studies that follow express a transgenic T cell receptor (TCR), DO11.10, which recognizes ovalbumin peptide presented by MHC class II [14]. Expression of a TCR transgene such as DO11.10 enhances both the health and longevity of IL-2 KO mice.

BALB/c DO11.10 mice expressing a transgenic IL-2 promoter/green fluorescent protein (GFP) reporter were the kind gift of Dr. Casey Weaver [15]. RAG-1 KO/DO11.10/IL-2 KO mice were produced by first generating RAG-1 KO/DO11.10/IL-2^{+/-} mice, breeding these mice, and then selecting for double knockout offspring. Mice were housed in specific pathogen free facilities and all experiments were in accordance with protocols approved by the University of Nebraska Institutional Animal Care and Use Committee.

For generation of bone marrow chimeras, RAG-1 KO or DO11.10/IL-2^{-/-} mice were irradiated with 5 Gy (Picker Cobalt 60 (V90) Teletherapy Unit). T cell depleted bone marrow was prepared from either DO11.10 WT or DO11.10/IL-2 KO mice and 7×10^6 cells were subsequently infused by tail vein injection into each animal. The majority of both the donor and recipient mice were female. Although reconstitution of the thymus with marrow expressing a TCR transgene alters the morphology of the medulla [16], it permits tracking of the

transplanted cells and controlled exposure to TCR-specific antigen. The transplanted cells may be tracked via the antibody KJ1-26, which recognizes the ova-specific TCR.

In situ hybridization

Thymic tissue was quick frozen on dry ice in OCT (Sakura Finetechnical Co., Tokyo, Japan) and stored at -80°C until use. Cryostat sections ($20\mu\text{m}$) were melted onto Superfrost Plus slides, air-dried for 30 min on 50°C slide warmer, and fixed in 4% paraformaldehyde for 15 min at 25°C . After washing the sections three times in PBS, microwave permeabilization was performed in 10mM citrate buffer pH 6.0 (Poly Scientific; Bay Shore, NY) at 90°C for 1 minute. The sections were incubated for 30 minutes at 37°C in pre-hybridization buffer. Slides were then incubated with 200 ng/ml of a digoxigenin-labeled, anti-sense probe cocktail for murine IL-2 (Gene Detect, Sarasota, FL) for 24 hr at 37°C . The cocktail consisted of three anti-sense probes recognizing non-overlapping regions within the coding sequence (NM 008366) of murine IL-2 mRNA as follows: probe 1 hybridized to nucleotides 250–297, probe 2 hybridized to nucleotides 328–375, and probe 3 hybridized to nucleotides 465–512. Post-hybridization stringency washes were performed with 1X SSC/10mM DTT (2×15 minutes at 55°C) and 0.5X SSC/10mM DTT (2×15 min at 55°C) and 10 minutes in 0.5X SSC/10mM DTT at room temperature. Sections were then washed in Roche washing buffer (Roche Molecular, Indianapolis, IN) and blocked in Roche blocking solution. Bound probe was detected using an AP-conjugated sheep anti-digoxigenin antibody (Roche) diluted 1:50 in blocking buffer and used overnight at 4°C . The slides were then rinsed with washing buffer, equilibrated in Roche detection buffer and immersed in BCIP/NBT liquid substrate (Sigma; St. Louis, MO). The reaction was stopped with several rinses of water and the sections covered in Aquamount (Lerner Lab, New Haven, CT). Control sections were probed with a cocktail of the corresponding sense probes and processed as described above.

Antibodies and flow cytometry

Single-cell suspensions were prepared from thymuses of bone marrow chimeras at 6–17 weeks post-transplantation. Cells ($1.5 \times 10^6/\text{ml}$) were stained for 30 minutes at 4°C with the fluorochrome-conjugated antibody of interest, then washed and resuspended in FACS buffer (PBS containing 2% v/v FBS and 0.1% NaN_3). Nonspecific binding was blocked prior to staining using Fc block (anti-CD16/32). Analysis was performed on a FACScan flow cytometer using CellQuest software (BD Biosciences, San Jose, CA). Anti-CD4 (RM4-5), CD8 (Ly-2), CD16/32 (2.4G2), and CD25 (PC61) were purchased from BD Pharmingen (San Diego, CA). Fluorochrome-conjugated KJ1-26 antibodies were from Caltag (Burlingame, CA).

Immunohistochemistry

Tissues were embedded in OCT, snap frozen in liquid nitrogen, and stored at -80°C until use. Cryostat sections ($5\mu\text{m}$) were prepared, fixed in acetone, and stained for IL-2 (using a rat anti-mouse IL-2 antibody, clone S4B6, BD Pharmingen) and/or 3G10. 3G10, a rat IgM mAb that recognizes medullary epithelium, was the kind gift of Dr. Andy Farr [17]. 3G10 was detected using a tetramethylrhodamine isothiocyanate-labeled anti-rat IgM antibody (Molecular Probes, Eugene, OR). Clone S4B6 was detected using a biotinylated rat anti-mouse secondary antibody (BD Pharmingen). Tyramine amplification methodology was then applied using streptavidin-horseradish peroxidase and tyramide-labeled fluorochromes per the manufacturer's recommendations (BD Pharmingen).

To ensure the specificity of S4B6, S4B6 was first pre-incubated overnight at 4°C with a 5M excess of murine IL-2 (BD Pharmingen) then used for staining as above.

Tissue sections from $\text{GFP}^{+/-}$ and $\text{GFP}^{-/-}$ mice were prepared as above then incubated in immunohistochemistry buffer [BupH PBS with 0.01% Tween-20, 0.1% saponin, and 1% w/v

blocking reagent (Molecular Probes T-20932)] for 16 hours at room temperature to decrease auto-fluorescence.

Tissue sections were mounted in Permount (Biomed, Foster City, CA) and visualized at room temperature using a Nikon Eclipse 80i microscope. A Plan Apo chromatic CF160-10X (aperture 0.45) objective was used. Images were captured using a Photometrics CoolSNAP CF camera and acquired using Metamorph image acquisition software.

Analysis of Ick and IL-2 proteins in tissues

To assess for thymic IL-2 by Western blot analysis, thymuses were homogenized in ice-cold 8M urea buffer (100 μ l buffer/mg tissue) containing 1mM PMSF (Sigma) and 0.05% Triton X-100 v/v. The homogenates were sonicated on ice, and then centrifuged to remove insoluble material. The resulting supernatants (extracts) were collected and an equal volume of 2X Laemmli running buffer (Bio-Rad, Hercules, CA) containing 5% β -mercaptoethanol (Bio-Rad) was added to each. The thymic extracts were separated by SDS-PAGE on 4–20% gradient gels (Bio-Rad), transferred to 0.2 μ m nitrocellulose, blocked with TTBS (Tris-buffered saline with 0.1% Tween-20) then probed for 16 hours with a rat anti-mouse IL-2 antibody (clone 18161D, BD Pharmingen). After washing with TTBS, bound antibody was detected with an alkaline phosphatase (AP)-conjugated goat anti-rat IgG (Zymax, San Francisco, CA). The blots were developed using enzyme chemiluminescence (Tropix, Bedford, MA) and blue X-ray film (Phenix, Hayward, CA).

To assess the phosphorylation state of thymic Ick, thymic homogenates were prepared by homogenizing thymuses in ice-cold Phosphosafe extraction buffer (Novagen, San Diego, CA) using 70 μ l buffer/mg tissue. The homogenates were sonicated on ice, insoluble material was pelleted by centrifugation, and the protein concentration of the resulting supernatants determined by DC protein assay (Bio-Rad). Seventy micrograms of each extract were separated by SDS-PAGE, transferred to 0.2 μ m nitrocellulose (not shown). The presence of a 56kD Ick band in the thymic homogenates was confirmed by Western blot analysis using a rabbit anti-Ick antibody (Abcam). To simultaneously identify Ick in each extract and assess the degree of phosphorylation of the Ick band, the blots were placed in a mini-protean II manifold blotter (Bio-Rad), permitting each lane to be probed with two different antibodies (left and right channels). The left channel of each lane was probed with a mouse anti-human Ick antibody (BD Pharmingen, 1:2000 in TTBS), while the right channel was probed with a biotinylated rabbit anti-phosphotyrosine antibody (Abcam, Cambridge, MA, 1:3000 in TTBS). The anti-Ick and anti-phosphotyrosine antibodies were detected with a goat-anti-mouse-AP (Zymax, San Francisco, CA, 1:4000 in TTBS) and avidin-AP (Sigma, 1:8000 in TTBS). The blots were developed as described above.

For immunoprecipitation of Ick, the aforementioned rabbit anti-Ick polyclonal antibody (Abcam) was conjugated to activated agarose using a commercially available immunoprecipitation kit (Pierce) resulting in approximately 75% coupling efficiency (determined spectrophotometrically). Thymic tissue extracts were prepared in Phosphosafe buffer as described above, and 350 μ g of each extract was suspended in 1 ml of precipitation binding buffer (Pierce) and incubated overnight with 15 μ g of anti-Ick conjugate. Precipitated Ick was pelleted by centrifugation, and after 5 washes with binding buffer was eluted from the anti-Ick conjugate with 2 washes of Immunopure elution buffer (Pierce). Each precipitate was suspended in an equal volume of Laemmli sample buffer (Bio-Rad), separated on a 10–20% gradient gel (Bio-Rad), transferred to nitrocellulose, and probed with the aforementioned biotinylated rabbit polyclonal anti-phosphotyrosine antibodies (Abcam) used at 1:3,000. The blots were then reacted with an avidin-HRP conjugate (InVitrogen) used at 1:8,000, then developed using an HRP chemiluminescence substrate (Pierce) and blue x-ray film (Phenix).

Analysis of DNA using PCR

The presence of IL-2, GFP, or actin DNA was detected by PCR as follows. DNA was isolated from thymuses and 300 ng were then subjected to PCR using *Taq* polymerase (Invitrogen, Carlsbad, CA) in combination with a forward primer specific for the IL-2 KO gene (neomycin gene inserted into the IL-2 gene - 5' TCGAATTCGCCAATGACAAGACGCT 3') or specific for the IL-2 WT gene (5' CTAGGCCACAGAATTGAAAGATCT 3') and a common reverse primer (5' GTAGGTGGAAATTCTAGCATCATCC 3'). PCR was performed in a GeneMate Magnum Thermocycler (ISC Bioexpress, Kaysville, UT) for 35 cycles (95°C for 3 min, 95°C for 25 sec, 60°C for 20 sec, 74°C for 25 sec, 74°C for 5 min). The KO IL-2 gene yields a 500bp product, and the WT IL-2 yields a 324 bp product. β -actin was amplified as an internal control and identified with the following primers: (5' ATCCCTGACCCTGAACTACCCATT3') and (3' GCACTGTAGTTTCTCTTCGACACGA 5'), and yielding a 240 bp product. GFP DNA was identified using the aforementioned protocol and the following primers: forward (5' AAGTTCATCTGCACCACCG 3') and reverse (5' TCCTTGAAGAAGATGGTGCG 3'), yielding a product of 173 bp.

Results

IL-2 KO mice acquire IL-2-expressing cells via maternal-fetal transmission

We first asked whether WT *IL2* DNA was detectable in IL-2 KO mice. Towards this end, we tested several organs of DO11.10/IL-2 KO mice for WT *IL2* DNA. WT *IL2* DNA was detected by PCR in the thymus (Figure 1a), spleen and lymph nodes (not shown) of DO11.10/IL-2 KO mice, suggesting that maternal cells had populated those tissues. WT *IL2* DNA was not found in heart, tail (Figure 1a) or skeletal muscle (not shown), suggesting that the DNA was from lymphoid cells.

To roughly compare the amount of *IL2* WT DNA present in IL-2 KO versus IL-2 WT tissues, DNA extracted from these thymuses was serially diluted and analyzed by PCR. *IL2* WT DNA from DO11.10/IL-2 KO thymuses was undetectable at a dilution of 1:50, whereas the *IL2* WT signal in DO11.10/IL-2 WT thymuses remained easily detectable in all dilutions (Figure 1a).

Given the presence of *IL2* WT DNA in IL-2 KO mice, we sought to localize IL-2 expressing cells by in situ hybridization. We looked for IL-2 mRNA rather than DNA in order to detect cells likely to be producing protein. In DO11.10/IL-2 WT thymuses, numerous cells containing IL-2 mRNA were distributed throughout the tissue (Figure 1b, left panel). In contrast, DO11.10/IL-2 KO thymuses exhibited occasional, small clumps of IL-2 positive cells, (approximately 2 per section; Figure 1b, right panel). These clumps may represent clones of IL-2-producing cells of maternal origin.

As an independent means of documenting the transfer of IL-2 producing cells from mother to offspring, we mated BALB/c DO11.10 females heterozygous for a transgenic IL-2 promoter/GFP reporter with BALB/c DO11.10 males and evaluated their GFP^{-/-} offspring for evidence of GFP⁺ cells. These mice were first stimulated for 24 hours with 10 μ g of anti-CD3 to enhance the production of GFP. GFP⁺ cells were observed in both thymus (Figure 1c) and spleen (not shown). In addition, GFP DNA was detected by PCR in the thymus and spleen but not in the heart or tail of GFP^{-/-} mice (not shown). Taken together, these results show that IL-2-producing cells are transferred from the mother to either IL-2 WT or IL-2 KO offspring.

Given that both WT *IL2* DNA and mRNA were detected in IL-2 KO mice, we next asked whether IL-2 protein was present in lymphoid tissues of IL-2 KO mice. Using a highly sensitive immunofluorescence detection method, tyramine amplification [18], we visualized IL-2 in the thymus and other lymphoid tissues of DO11.10/IL-2 KO mice. Interestingly, a substantial amount of the IL-2 was localized to the thymic medulla (Figure 2a), a region thought to be

critical to negative selection [19]. Controls, including secondary antibody alone (not shown) and pre-incubation of the primary antibody with a five-molar excess of IL-2 (Figure 2b), were negative. Tissues, such as muscle, which would not be expected to have IL-2 producing cells, were also negative (Figure 2b). In support of the above immunostaining results, we were also able to detect IL-2 by Western blot analysis in thymuses of DO11.10/IL-2 KO mice (Figure 2c).

Thymic morphology is abnormal in IL-2 deficiency

To determine whether the IL-2 present in IL-2 KO mice might alter their thymic function, we sought to generate a model of complete or nearly complete IL-2 deficiency. Towards this end, we irradiated RAG-1^{-/-} mice and reconstituted their immune systems by transplantation of either DO11.10/IL-2 WT or DO11.10/IL-2 KO bone marrow. Development of both thymocytes and thymic stroma is arrested in RAG-1^{-/-} mice, but reconstitution of the immune system with WT bone marrow allows development to proceed beyond this arrest to yield a normal thymus [20]. Although RAG-1^{-/-} mice have the ability to produce IL-2, this production is markedly decreased due to a lack of mature T cells in the thymus and periphery. Hence, RAG-1^{-/-} mice reconstituted with marrow from DO11.10/IL-2 KO mice should have little or no IL-2 (as irradiation will not remove retained IL-2 protein), without the ability to produce any additional IL-2.

To assess the severity of IL-2 deficiency in DO11.10/IL-2 KO/RAG-KO bone marrow chimeras, we examined thymuses at several time points after reconstitution for the presence of IL-2. As seen in Figure 3, IL-2 was nearly undetectable 17 weeks post-reconstitution.

We then asked whether the morphology of the thymus was altered in the near absence of IL-2. By 12 – 17 weeks post reconstitution, the entire thymus was decreased in size in RAG-1 KO mice that received DO11.10/IL-2 KO marrow (not shown). The thymic medulla was especially atrophied, and in some cases it was absent altogether (Figure 3). These results suggest that IL-2, either via a direct influence on medullary epithelium or indirectly via an influence on thymocytes, is important in maintaining the thymic medulla.

Thymic reconstitution in an IL-2 deficient environment is abnormal

During thymic development or upon reconstitution of an ablated immune system, lymphoid precursors enter the thymus and progress through distinct stages, defined primarily by the expression of CD4 and CD8. Given the morphologic abnormalities noted above, we next asked whether thymocyte populations were altered in severe IL-2 deficiency. As seen in Figure 4, the frequency of CD4⁺CD8⁺ thymocytes generated from DO11.10/IL-2 KO marrow, while initially higher than the frequency of CD4⁺CD8⁺ thymocytes generated from DO11.10/IL-2 WT marrow, decreased with time post-transplantation until this population was almost gone. Examination of CD4⁺KJ1-26⁺ populations within the same mice revealed a decline in the frequency of less mature, CD4⁺KJ1-26^{lo} T cells and an increase in the frequency of CD4⁺KJ1-26^{hi} T cells as time progressed post-transplantation. This gradual loss of CD4⁺KJ1-26^{lo} and CD4⁺CD8⁺ thymocytes correlated with the size of the thymus (Figure 4a). These findings suggest that in severe IL-2 deficiency, the thymus gradually loses cellularity and differentially loses CD4⁺CD8⁺ and CD4⁺TCR^{lo} thymocytes.

Results similar to those in Figure 4 were obtained when DO11.10/IL-2 KO bone marrow was transferred into lethally irradiated, DO11.10/IL-2 KO mice. Transfer of DO11.10/IL-2 WT marrow into DO11.10/IL-2 KO mice corrected these abnormalities (data not shown). DO11.10/IL-2 KO mice in our colony also exhibit a gradual loss of CD4⁺CD8⁺ thymocytes and thymic medulla, but these changes occur over a period of 6 to 7 months rather than 12–17 weeks.

A gradual loss of CD4⁺CD8⁺ thymocytes has been noted in several strains of mice that develop autoimmunity [21]. Because a similar pattern occurs acutely in mice under physiologic stress [22], loss of CD4⁺CD8⁺ thymocytes in autoimmunity has been attributed to autoimmune-mediated stress [6]. To determine whether the loss of CD4⁺CD8⁺ thymocytes in severe IL-2 deficiency was related to autoimmunity, we generated RAG-KO/DO11.10/IL-2 KO mice. These mice produce only T cells with a T cell receptor that recognizes ovalbumin, and therefore they do not develop autoimmunity. RAG-KO/DO11.10/IL-2 KO mice, as compared to RAG-KO/DO11.10/IL-2 WT mice, also exhibited a decrease in their CD4⁺CD8⁺ thymocyte population with time (Figure 5), suggesting that the gradual loss of this double positive population is due to an absence of IL-2 rather than autoimmune stress.

Generation of CD8⁺KJ1-26⁺ T cells in IL-2 deficiency

Examination of peripheral lymphocytes in DO11.10/IL-2 KO→RAG-KO chimeras revealed a significant population of CD8⁺KJ1-26⁺ T cells. Twenty-four percent of KJ1-26⁺ splenocytes or lymphocytes in the DO11.10/IL-2 KO→RAG-KO chimeras were CD8⁺ as compared to 5% in the DO11.10/IL-2 WT→RAG-KO chimeras (Figure 6). Because the DO11.10 TCR recognizes ovalbumin peptide presented by MHC class II, very few of the KJ1-26⁺ T cells are CD8⁺, as demonstrated by the WT controls. In order to determine whether generation of CD8⁺KJ1-26⁺ thymocytes contributed to the high frequency of CD8⁺KJ1-26⁺ T cells found in the periphery, we examined the frequencies of CD8⁺KJ1-26⁺ thymocytes in our bone marrow chimeras. As seen in Figure 7, the frequency of CD8⁺ T cells within the KJ1-26⁺ T cell population increased with time in RAG-1^{-/-} mice receiving DO11.10/IL-2 KO marrow. Although some of the skewed TCRs are likely to be hybrids of the transgenic β chain and the endogenous α chain [23], nevertheless these T cells express CD8 in the absence of IL-2 and CD4 in its presence. Whether these cells perform like CD8⁺ cells, as determined by expression of lineage-specific genes and functional assays, is under investigation. We also examined the frequency of KJ1-26⁺CD8⁺ thymocytes in RAG-KO/DO11.10/IL-2 KO mice, which have no capacity for endogenous TCR rearrangement. Thymocytes in these mice also exhibited an increased frequency of KJ1-26⁺CD8⁺ cells, as compared to RAG-KO/DO11.10/IL-2 WT mice, although the frequency of these cells was much lower than that seen in the bone marrow chimeras (manuscript in preparation).

Phosphorylation of lck is decreased in an IL-2 deficient environment

We next began to explore possible mechanisms behind the decline in CD4⁺CD8⁺ thymocytes and increase in KJ1-26⁺CD8⁺ thymocytes evident in the DO11.10/IL-2 KO→RAG-KO chimeras and RAG-KO/DO11.10/IL-2KO mice. Similar to these severely IL-2 deficient mice, lck^{-/-} mice exhibit a decrease in CD4⁺CD8⁺ thymocytes over time [24]. Lck also influences lineage commitment, and decreased activation of lck skews commitment towards the CD8 lineage [25]. Although activation of lck during lineage commitment is thought to occur primarily by association with CD4 or CD8, lck can also be activated via IL-2Rβ[26,27]. Given this information, we asked whether the activation of lck is decreased in the absence of IL-2. To address this question, thymic tissue homogenates were prepared from RAG-1^{-/-} thymuses 12 weeks after reconstitution with either DO11.10/IL-2 KO or DO11.10/IL-2 WT marrow. As seen in Figure 8a, the thymic homogenates contained a band of the appropriate molecular weight (~56 kD) that was recognized by an anti-lck antibody. Western blot analysis with an anti-phospho-tyrosine antibody revealed that the phosphorylation state of thymic lck was diminished in thymuses reconstituted with DO11.10/IL-2 KO versus DO11.10/IL-2 WT marrow (Figure 8b).

To ensure that the decreased phosphorylation of lck noted above was not due to the altered frequencies of thymocyte subpopulations in 12-week old DO11.10/IL-2 KO→RAG-KO bone marrow chimeras, we assessed the phosphorylation of lck in 6-week old DO11.10/IL-2 WT

and KO thymuses by immunoprecipitation of Ick. Similar to the bone marrow chimeras (Figure 4), the frequency of CD4⁺CD8⁺ thymocytes in these younger mice was slightly higher in the DO11.10/IL-2 KO mice than in the DO11.10/IL-2 WT mice (81% and 71% respectively). As seen in Figure 8c, even in younger mice with similar compositions of thymocytes, the phosphorylation of Ick was diminished in DO11.10/IL-2 KO vs DO11.10/IL-2 WT mice.

Finally, we asked whether the administration of IL-2 to IL-2 KO mice would increase the phosphorylation of Ick. For this experiment, older (≥ 10 weeks) DO11.10/IL-2 KO mice were chosen as they exhibit much less retained IL-2. As seen in Figure 8d, phosphorylation of Ick was substantially greater in mice that received IL-2 versus carrier alone. In summary, our findings suggest that signaling via the IL-2 receptor contributes to the phosphorylation (i.e., activation) of Ick in the thymus.

Discussion

This report details two findings of significance. First, IL-2 is present in IL-2 KO mice in amounts sufficient to alter the thymic phenotype of IL-2 KO mice, thus obscuring the influence of IL-2 on thymic function. Second, this IL-2 is acquired via seeding of IL-2 KO fetuses with IL-2 producing cells from their heterozygous mothers.

Maternal cells are always found in fetuses when detection methods of sufficient sensitivity are used [12,13]. Using PCR, Marleau et al. found that murine fetuses have maternal cells in their bone marrow. After birth, these cells persisted for up to 12 weeks in the spleen [13]. Zhou et al. detected maternal cells by flow cytometry or histology in the thymuses, livers, and spleens of 18-day gestation fetuses [28]. They also showed that maternally-derived cells were transferred via breast milk to the liver.

Our data (Figures 1, 2) suggest that maternally-derived cells persist in the spleen and thymus, and can produce IL-2 in amounts sufficient to alter the phenotype of IL-2 KO mice. Through the generation of DO11.10/IL-2 KO \rightarrow RAG-1 KO chimeras, we demonstrate that IL-2 influences several aspects of thymocyte differentiation and the maintenance of a normal thymic medulla. In a broader sense, our results show that the phenotype of genetic KO mice does not necessarily reflect a loss of function of the deleted gene. The maternal transfer of cytokines/growth factors, either directly by transmission of the cytokine or indirectly via transfer of cytokine-producing cells, likely modifies the phenotype of other animal models. In particular, maternal transfer of TGF β -1 protein has been shown to influence the survival of TGF β -1 KO newborns [29].

Our findings, combined with those of other investigators, help clarify how IL-2 functions in the maintenance of the postnatal thymus. Schorle et al. [5], and Reya, et al [30] found that the distribution of thymocyte populations was normal in 4 week-old, IL-2 KO mice. However, Reya found that the number of double positive thymocytes was greatly decreased by 8 weeks of age [30]. IL-2R β KO mice also exhibited a significant decline in their double positive population, which was not evident at 3 weeks of age but clearly present by 6 weeks [6]. Given the autoimmune phenotype of IL-2 or IL-2 receptor deficient mice, autoimmune stress was posited in both of these studies to be a possible cause for the decline in double positive thymocytes.

Our results with RAG-KO/DO11.10/IL-2 KO mice, which do not develop autoimmunity, suggest that the decline in double positive thymocytes is due to the absence of IL-2 rather than autoimmune stress. Several autoimmune strains of mice, including MRL-*lpr/lpr*, NOD, BXSB, and NZB, develop a decreased CD4⁺CD8⁺ thymocyte population with time [21,31]. Interestingly, MRL-*lpr/lpr* mice and NOD mice, which are murine models for lupus and Type 1 diabetes respectively, both exhibit a hypoactive variant of IL-2 [32,33]. In addition, IL-2

production is decreased in these mice [34,35] as well as in both NZB mice and BXSb males [36–38]. BXSb females, which do not develop autoimmunity or a decline in CD4⁺CD8⁺ thymocytes, do not exhibit a decrease in IL-2 production [38]. We hypothesize that decreased activation of the tyrosine kinase lck, via reduced IL-2R β signaling, contributes to a decline in CD4⁺CD8⁺ thymocytes. In the context of CD4⁺CD8⁺ thymocytes, lck^{-/-} mice are similar to IL-2 KO and IL-2R β KO mice, in that the lck^{-/-} mice do not exhibit a large decrease in their double positive population until after 2 weeks of age [39].

The transitions from CD4⁻CD8⁻ to CD4⁺CD8⁺, and from CD4⁺CD8⁺ to CD4⁺ or CD8⁺ T cells, are both influenced by lck [24,39–41]. In CD4⁺CD8⁺ thymocytes, lck activity influences both the maturation of thymocytes to the single positive stage and their commitment to either the CD4 or CD8 lineage [25,41–43]. Although lck signaling during lineage commitment is thought to arise largely from association with intracellular CD4 and CD8 [27], lck also associates with IL-2R β [26]. Our studies indicating that the phosphorylation of tyrosine residues in lck is decreased in IL-2 deficiency, and that administration of IL-2 increases phosphorylation of lck in IL-2 KO mice, suggest that signaling via IL-2R β contributes to the total activation of lck during thymocyte development.

Although the maternally-derived cells transferred to the IL-2 KO offspring may only produce a small amount of IL-2, that IL-2 is in effect “concentrated” by its retention in the extracellular matrix via heparan sulfate [44,45]. Our work in this regard has focused on the spleen, in which heparan sulfate-bound IL-2 is localized to the red pulp and marginal zones. In the thymus, IL-2 appears to be localized to thymocyte cell surfaces and medullary epithelium (Figures 2 and 3). In contrast to the spleen, in which immunohistochemical detection of IL-2 is diminished by heparitinase digestion [44], our preliminary data indicate that detection of IL-2 is enhanced by heparitinase digestion of thymic tissue sections. While both these data suggest that IL-2 is closely associated with heparan sulfate, the nature of this association may differ between the two organs.

In summary, our findings indicate that “true” IL-2 deficiency impacts the morphology and function of the thymus. Inconsistencies with respect to the role of IL-2 in both central and peripheral immunity may be explained by our finding that IL-2 KO mice contain maternally-derived cells that produce IL-2 and, consequently, exhibit varying levels of retained IL-2 in their tissues. This retained IL-2 clearly impacts the phenotype of IL-2 KO mice; furthermore, the means by which these mice acquire IL-2 may be applicable to other KO models. The generation of fertile IL-2 KO females will be necessary to discern the true phenotype resulting from absence of IL-2.

Acknowledgements

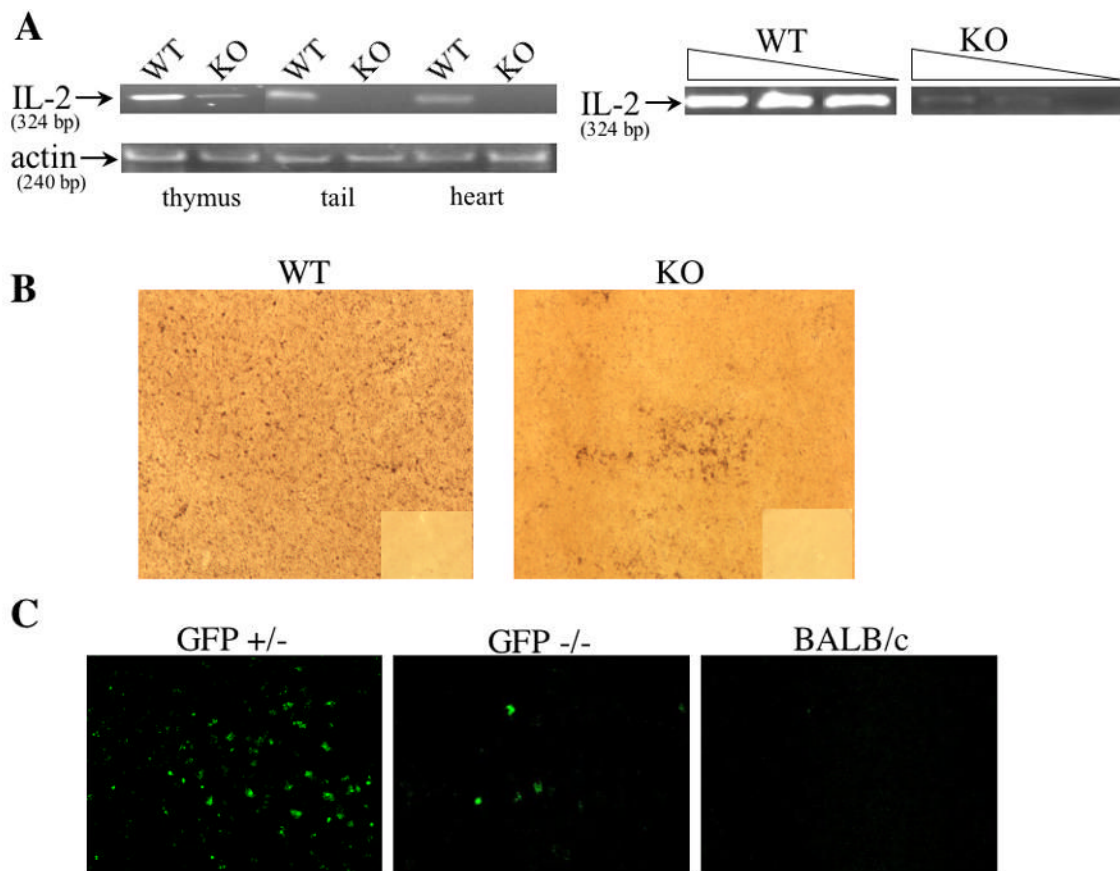
We thank Dr. Marianne Mannion for performing the PCR studies and Mr. Frederick Potmesil for assistance with Western blots. We also thank the Cell Analysis Facility at the University of Nebraska Medical Center for performing the data acquisition portion of the flow cytometry studies.

References

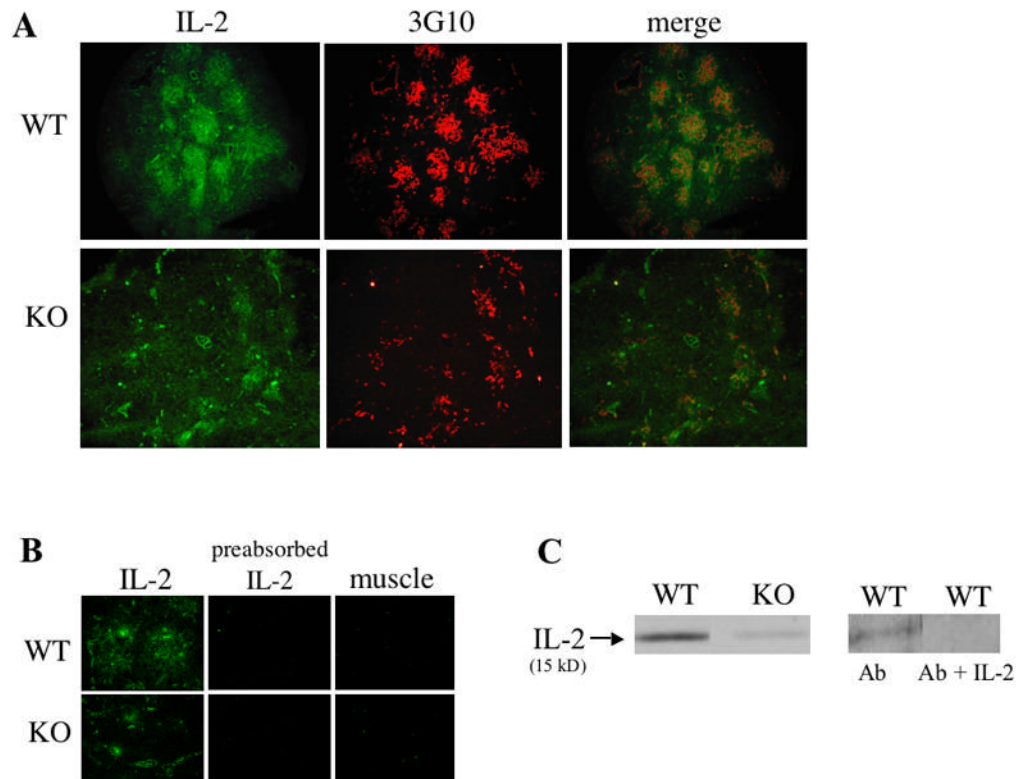
1. Yang-Snyder JA, Rothenberg EV. Developmental and anatomical patterns of IL-2 gene expression in vivo in the murine thymus. *Dev Immunol* 1993;3:85–102. [PubMed: 8298302]
2. Rothenberg EV, Diamond RA, Chen D. Programming for recognition and programming for response. Separate developmental subroutines in the murine thymus. *Thymus* 1994;22:215–244. [PubMed: 7985222]
3. Carding SR, Jenkinson EJ, Kingston R, Hayday AC, Bottomly K, Owen JJ. Developmental control of lymphokine gene expression in fetal thymocytes during T-cell ontogeny. *Proc Natl Acad Sci USA* 1989;86:3342–3345. [PubMed: 2497464]

4. Willerford DM, Chen J, Ferry JA, Davidson L, Ma A, Alt FW. Interleukin-2 receptor alpha chain regulates the size and content of the peripheral lymphoid compartment. *Immunity* 1995;3:521–530. [PubMed: 7584142]
5. Schorle H, Holtschke T, Hunig T, Schimpl A, Horak I. Development and function of T cells in mice rendered interleukin-2 deficient by gene targeting. *Nature* 1991;352:621–624. [PubMed: 1830926]
6. Suzuki H, Kundig TM, Furlonger C, Wakeham A, Timmes E, Matsuyama T, Schmits R, Simard JJ, Ohashi PS, Griesser H, Taniguchi T, Paige CJ, Mak TW. Deregulated T cell activation and autoimmunity in mice lacking interleukin-2 receptor beta. *Science* 1995;268:1472–1476. [PubMed: 7770771]
7. Jenkinson EJ, Kingston R, Owen JJ. Importance of IL-2 receptors in intra-thymic generation of cells expressing T-cell receptors. *Nature* 1987;329:160–162. [PubMed: 3114642]
8. Bassiri H, Carding SR. A requirement for IL-2/IL-2 receptor signaling in intrathymic negative selection. *J Immunol* 2001;166:5945–5954. [PubMed: 11342609]
9. Plum J, De Smedt M. Differentiation of thymocytes in fetal organ culture: lack of evidence for the functional role of the interleukin 2 receptor expressed by prothymocytes. *Eur J Immunol* 1988;18:795–799. [PubMed: 3132397]
10. Kramer S, Schimpl A, Hunig T. Immunopathology of interleukin (IL) 2-deficient mice: thymus dependence and suppression by thymus-dependent cells with an intact IL-2 gene. *J Exp Med* 1995;182:1769–1776. [PubMed: 7500021]
11. Kramer S, Mamalaki C, Horak I, Schimpl A, Koussis D, Hung T. Thymic selection and peptide-induced activation of T cell receptor-transgenic CD8 T cells in interleukin-2-deficient mice. *Eur J Immunol* 1994;24:2317–2322. [PubMed: 7925559]
12. Petit T, Dommergues M, Socie G, Dumez Y, Gluckman E, Brison O. Detection of maternal cells in human fetal blood during the third trimester of pregnancy using allele-specific PCR amplification. *Br J Haematol* 1997;98:767–771. [PubMed: 9332337]
13. Marleau AM, Greenwood JD, Wei Q, Singh B, Croy BA. Chimerism of murine fetal bone marrow by maternal cells occurs in late gestation and persists into adulthood. *Lab Invest* 2003;83:673–681. [PubMed: 12746477]
14. Murphy KM, Heimsberger AB, Loh DY. Induction by antigen of intrathymic apoptosis of CD4⁺CD8⁺TCR^{lo} thymocytes in vivo. *Science* 1990;250:1720–1723. [PubMed: 2125367]
15. Saparov A, Wagner FH, Zheng R, Oliver JR, Maeda H, Hockett RD, Weaver CT. Interleukin-2 expression by a subpopulation of primary T cells is linked to enhanced memory/effector function. *Immunity* 1999;11:217–280.
16. Brabb T, Huseby ES, Morgan TM, Sant' Angelo DB, Kirchner J, Farr AG, Goverman J. Thymic stromal organization is regulated by the specificity of T cell receptor/major histocompatibility complex interactions. *Eur J Immunol* 1997;27:136–146. [PubMed: 9022010]
17. Anderson M, Anderson SK, Farr AG. Thymic vasculature: organizer of the medullary epithelial compartment? *Int Immunol* 2000;12:1105–1110. [PubMed: 10882422]
18. Toda Y, Kono K, Abiru H, Kokuryo K, Endo M, Yaegashi H, Fukumoto M. Application of tyramide signal amplification system to immunohistochemistry: a potent method to localize antigens that are not detectable by ordinary method. *Pathol Int* 1999;49:479–483. [PubMed: 10417696]
19. Kishimoto H, Sprent J. Several different cell surface molecules control negative selection of medullary thymocytes. *J Exp Med* 1999;190:65–73. [PubMed: 10429671]
20. van Ewijk W, Hollander G, Terhorst C, Wang B. Stepwise development of thymic microenvironments in vivo is regulated by thymocyte subsets. *Development* 2000;127:1583–1591. [PubMed: 10725235]
21. Kakkanaiah VN, Pyle RH, Nagarkatti M, Nagarkatti PS. Evidence for major alterations in the thymocyte subpopulations in murine models of autoimmune diseases. *J Autoimmun* 1990;3:271–288. [PubMed: 1975741]
22. Hirahara H, Ogawa M, Kimura M, Iiai T, Tsuchida M, Hanawa H, Watanabe H, Abo T. Glucocorticoid independence of acute thymic involution induced by lymphotoxin and estrogen. *Cell Immunol* 1994;153:401–411. [PubMed: 8118872]
23. Hurst SD, Sitterding SM, Ji S, Barrett TA. Functional differentiation of T cells in the intestine of T cell receptor transgenic mice. *Proc Natl Acad Sci USA* 1997;94:3920–3921. [PubMed: 9108080]

24. Molina TJ, Kishihara K, Siderovski DP. Profound block in thymocyte development in mice lacking p56^{lck}. *Nature* 1992;357:161–164. [PubMed: 1579166]
25. Hernandez-Hoyos G, Sohn SJ, Rothenberg EV, Alberola-Ila J. Lck activity controls CD4/CD8 T cell lineage commitment. *Immunity* 2000;12:313–322. [PubMed: 10755618]
26. Minami Y, Kono T, Yamada K, Kobayashi N, Kawahara A, Perlmutter RM, Taniguchi T. Association of p56lck with IL-2 receptor beta chain is critical for the IL-2-induced activation of p56lck. *EMBO J* 1993;12:759–768. [PubMed: 8440263]
27. Trobridge PA, Forbush KA, Levin SD. Positive and negative selection of thymocytes depends on lck interaction with the CD4 and CD8 coreceptors. *J Immunol* 2001;166:809–818. [PubMed: 11145654]
28. Zhou L, Yoshimura Y, Huang YY, Suzuki R, Yokoyama M, Okabe M, Shimamura M. Two independent pathways of maternal cell transmission to offspring: through placenta during pregnancy and by breast-feeding after birth. *Immunology* 2000;101:570–580. [PubMed: 11122462]
29. Letterio JJ, Geiser AG, Kulkarni AB, Roche NS, Sporn MB, Roberts AB. Maternal rescue of transforming growth factor-beta 1 null mice. *Science* 1994;264:1936–1938. [PubMed: 8009224]
30. Reya T, Bassiri H, Biancaniello R, Carding SR. Thymic stromal-cell abnormalities and dysregulated T-cell development in IL-2-deficient mice. *Dev Immunol* 1998;5:287–302. [PubMed: 9814585]
31. Zhang ZL, Constantinou D, Mandel TE, Georgiou HM. Lymphocyte subsets in thymus and peripheral lymphoid tissues of aging and diabetic NOD mice. *Autoimmunity* 1994;17:41–48. [PubMed: 8025213]
32. Choi Y, Simon-Stoos K, Puck JM. Hypo-active variant of IL-2 and associated decreased T cell activation contribute to impaired apoptosis in autoimmune prone MRL mice. *Eur J Immunol* 2002;32:677–685. [PubMed: 11857342]
33. Matesanz F, Alcina A. High expression in bacteria and purification of polymorphic mouse interleukin 2 molecules. *Cytokine* 1998;10:249–253. [PubMed: 9617568]
34. Serreze DV, Leiter EH. Defective activation of T suppressor cell function in nonobese diabetic mice. *J Immunol* 1988;140:3801–3807. [PubMed: 2897395]
35. Altman A, Theofilopoulos AN, Weiner R, Katz DH, Dixon FJ. Analysis of T cell function in autoimmune murine strains. *J Exp Med* 1981;154:791–808. [PubMed: 6456321]
36. Chu EB, Ernst DN, Hobb MV, Weigle WO. Maturation changes in CD4⁺ cell subsets and lymphokine production in BXSB Mice. *J Immunol* 1994;152:4129–4138. [PubMed: 7511669]
37. Sato MN, Minoprio P, Avrameas S, Ternynck T. Defects in the regulation of anti-DNA antibody production in aged lupus-prone (NZB × NZW)F1 mice, analysis of T-cell lymphokine synthesis. *Immunology* 1995;85:26–32. [PubMed: 7635519]
38. Lin LC, Chen YC, Chou CC, Hsieh KH, Chiang BL. Dysregulation of T helper cell cytokines in autoimmune prone NZB × NZW F1 mice. *Scand J Immunol* 1995;42:466–472. [PubMed: 7569780]
39. Molina TJ, Perrot J, Penninger J, Ramos A, Audouin J, Briand P, Mak TW, Diebold J. Differential requirement for p56lck in fetal and adult thymopoiesis. *J Immunol* 1998;160:3828–3834. [PubMed: 9558087]
40. Anderson SJ, Levin SD, Perlmutter RM. Protein tyrosine kinase p56lck controls allelic exclusion of T-cell receptor beta-chain genes. *Nature* 1993;365:552–554. [PubMed: 8413611]
41. Sohn SJ, Forbush KA, Pan XC, Perlmutter RM. Activated p56lck directs maturation of both CD4 and CD8 single-positive thymocytes. *J Immunol* 2001;166:2209–2217. [PubMed: 11160274]
42. Singer A. New perspectives on a developmental dilemma: the kinetic signaling model and the importance of signal duration for the CD4/CD8 lineage decision. *Curr Opin Immunol* 2002;14:207–215. [PubMed: 11869894]
43. Germain RN. T-cell development and the CD4-CD8 lineage decision. *Nat Rev Immunol* 2002;2:309–322. [PubMed: 12033737]
44. Wrenshall LE, Platt JL. Regulation of T cell homeostasis by heparan sulfate-bound IL-2. *J Immunol* 1999;163:3793–3800. [PubMed: 10490977]
45. Wrenshall LE, Platt JL, Stevens ET, Wight TN, Miller JD. Propagation and control of T cell responses by heparan sulfate-bound IL-2. *J Immunol* 2003;170:5470–5474. [PubMed: 12759423]

**Figure 1.**

Detection of IL-2 DNA and IL-2 producing cells in IL-2 KO offspring of IL-2 heterozygous mothers. (A) Analysis of *IL2* WT DNA in IL-2 KO mice. DNA was extracted from the thymus, heart, and tail of DO11.10/IL-2 WT or DO11.10/IL-2 KO mice and 300 ng were then used to detect the presence/absence of *IL2* WT gene via PCR. β -actin was used as a loading control. In a separate experiment, DNA extracted from either DO11.10/IL-2 WT or DO11.10/IL-2 KO thymuses was serially diluted (undiluted, 1:10, 1:50) then assayed via PCR. (B) Thymic tissue sections from DO11.10/IL-2 KO offspring of DO11.10/IL-2 heterozygous mothers were processed for in situ hybridization, and IL-2 message was detected using a digoxigenin-labeled oligonucleotide probe cocktail for murine IL-2 mRNA (magnification 10x). The corresponding sense controls are shown in the right lower quadrant of each picture. (C) Thymic tissue sections from GFP^{-/-} offspring of GFP^{+/-} mothers expressing a transgenic IL-2 promoter/GFP reporter were assessed for the presence of GFP⁺ cells (magnification 10x). Sections from BALB/c mice were used as a negative control. Data shown in each figure are representative of several sections from 2 different animals.

**Figure 2.**

Detection of IL-2 protein in IL-2 WT and KO thymuses. (A) Cryosections of DO11.10/IL-2^{+/+} or DO11.10/IL-2^{-/-} thymuses were stained for IL-2 (fluorescein isothiocyanate) and medullary epithelium (tetramethylrhodamine isothiocyanate) using clone 3G10 (magnification 10x). (B) Cryosections of DO11.10/IL-2^{+/+} or DO11.10/IL-2^{-/-} thymuses or muscle were stained with a rat anti-mouse monoclonal antibody recognizing IL-2. To ensure specificity of the antibody, additional sections of thymus were stained with anti-IL-2 antibodies incubated with a 5M excess of IL-2 (preabsorbed IL-2). (C) Analysis of IL-2 protein by Western blot in DO11.10/IL-2 KO mice. Total protein was extracted from 1 thymic lobe of DO11.10/IL-2 WT or DO11.10/IL-2 KO mice, then separated by SDS-PAGE, transferred to nitrocellulose, and probed with anti-IL-2 antibodies. Pre-absorption of the primary anti-IL-2 antibody (Ab) with an excess of recombinant murine IL-2 (Ab + IL-2) showed no labeling.

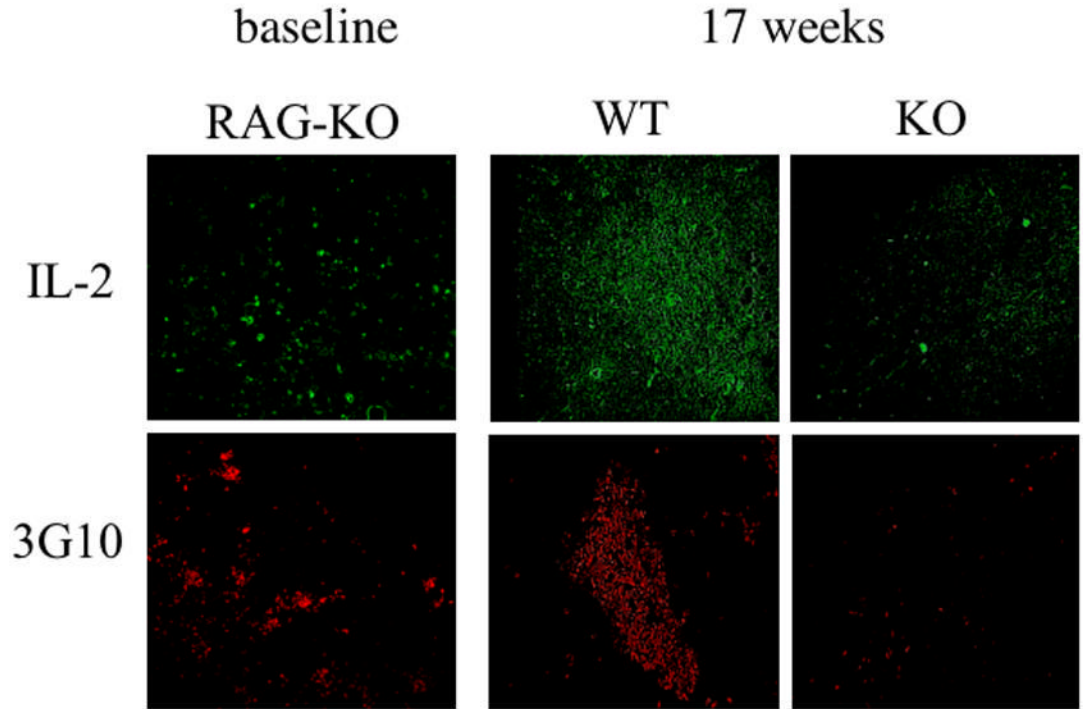
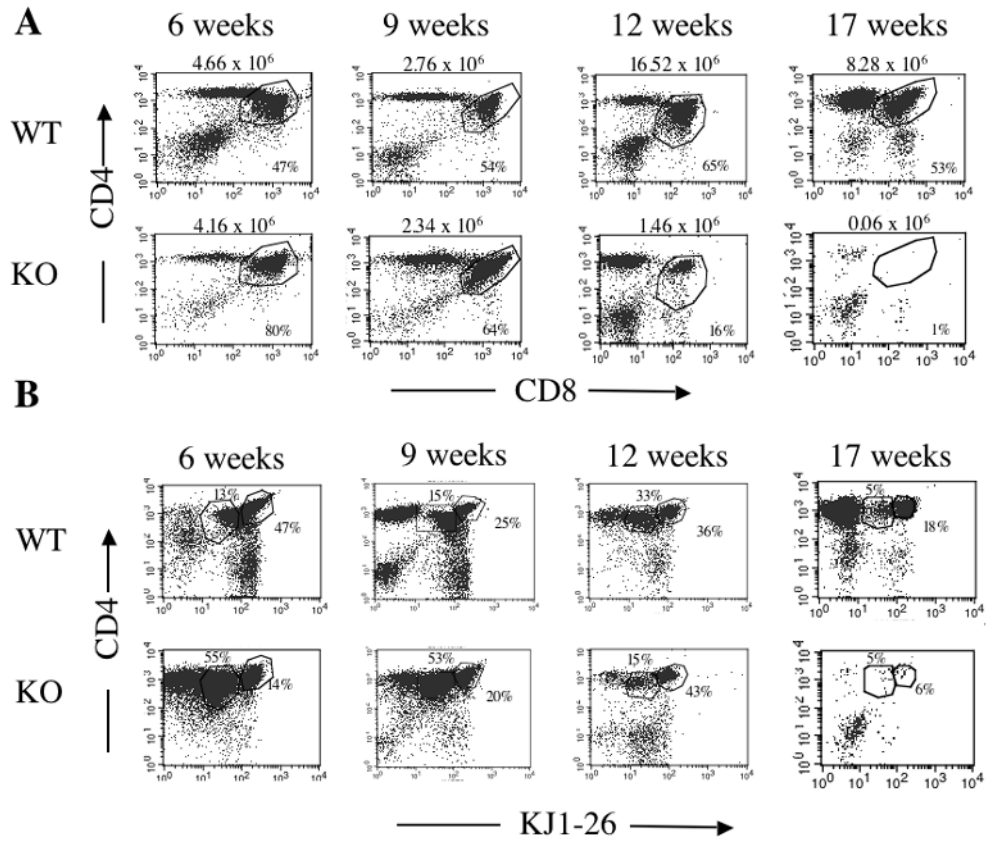


Figure 3.

Thymic morphology of thymuses from RAG-1^{-/-} mice reconstituted with either DO11.10/IL-2 WT or DO11.10/IL-2 KO bone marrow. Cryosections of thymuses from the above mice were analyzed at 17 weeks post-transplantation and stained with antibodies recognizing IL-2 and medullary epithelium (3G10). Secondary antibodies and reagents for tyramine amplification (for IL-2) were then applied. Thymuses of untreated, RAG-1 KO mice are shown as a baseline (magnification 10x).

**Figure 4.**

Serial assessment of thymocyte populations in RAG-1^{-/-} mice reconstituted with either DO11.10/IL-2 WT or DO11.10/IL-2 KO bone marrow. Thymocytes, prepared from mice 6 - 17 weeks post-transplantation, were analyzed by flow cytometry for the presence of (A) CD4 and CD8, or (B) KJ1-26 and CD4. The numbers above the dot plots in (A) represent the number of cells in the thymus from which the dot plot originated. Data shown are representative of 3 or more experiments, with 3 animals per group. Data from the 17-week group are representative of 1 experiment, with 6 animals per group.

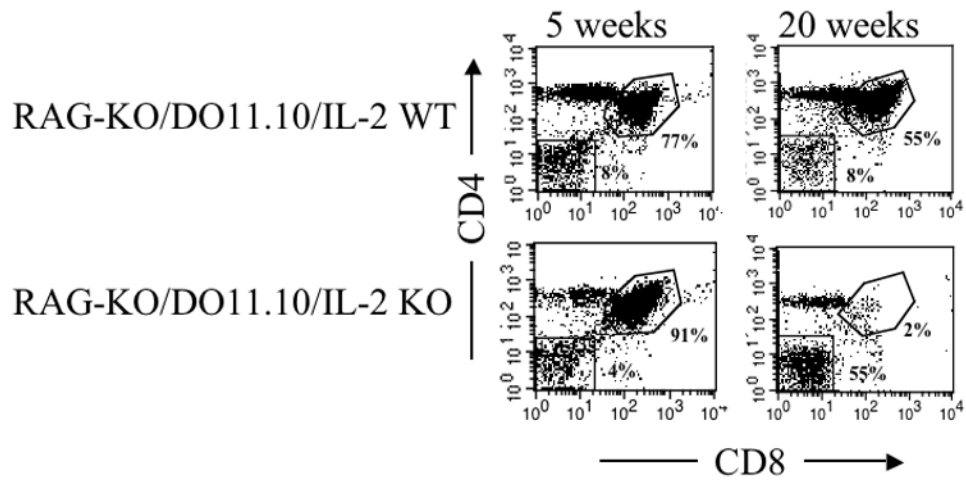


Figure 5.

Change in frequency of CD4⁺CD8⁺ thymocytes, with age, in RAG-KO/DO11.10/IL-2 KO mice. Thymocytes, prepared from 5 or 20 week-old RAG-KO/DO11.10/IL-2 WT or RAG-KO/DO11.10/IL-2 KO mice, were analyzed by flow cytometry for the presence of CD4 and CD8. Data shown are representative of 3 pairs of mice of similar ages.

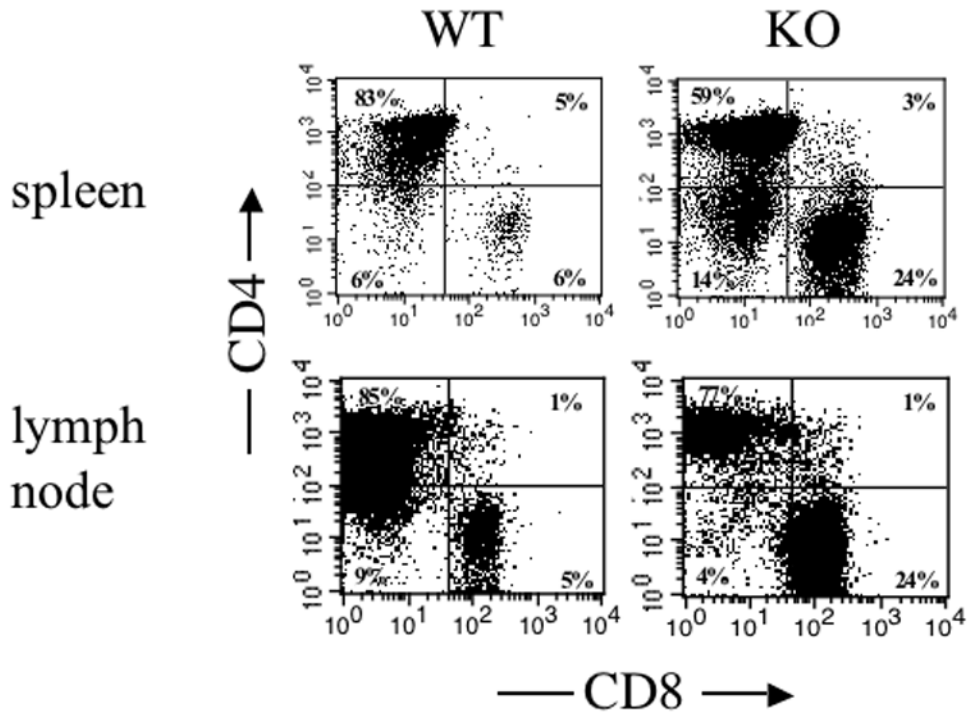


Figure 6.

Phenotype of lymphocyte populations in the spleen and lymph nodes of RAG-1^{-/-} mice reconstituted with either DO11.10/IL-2 WT or DO11.10/IL-2 KO bone marrow. Lymphocytes, prepared from the above organs of mice 12 weeks post-transplantation, were analyzed by flow cytometry for the frequency of CD4⁺, CD8⁺ or CD4⁺CD8⁺ cells within the KJ1-26⁺ population. Data shown are representative of 3 or more experiments, with 3 animals per group.

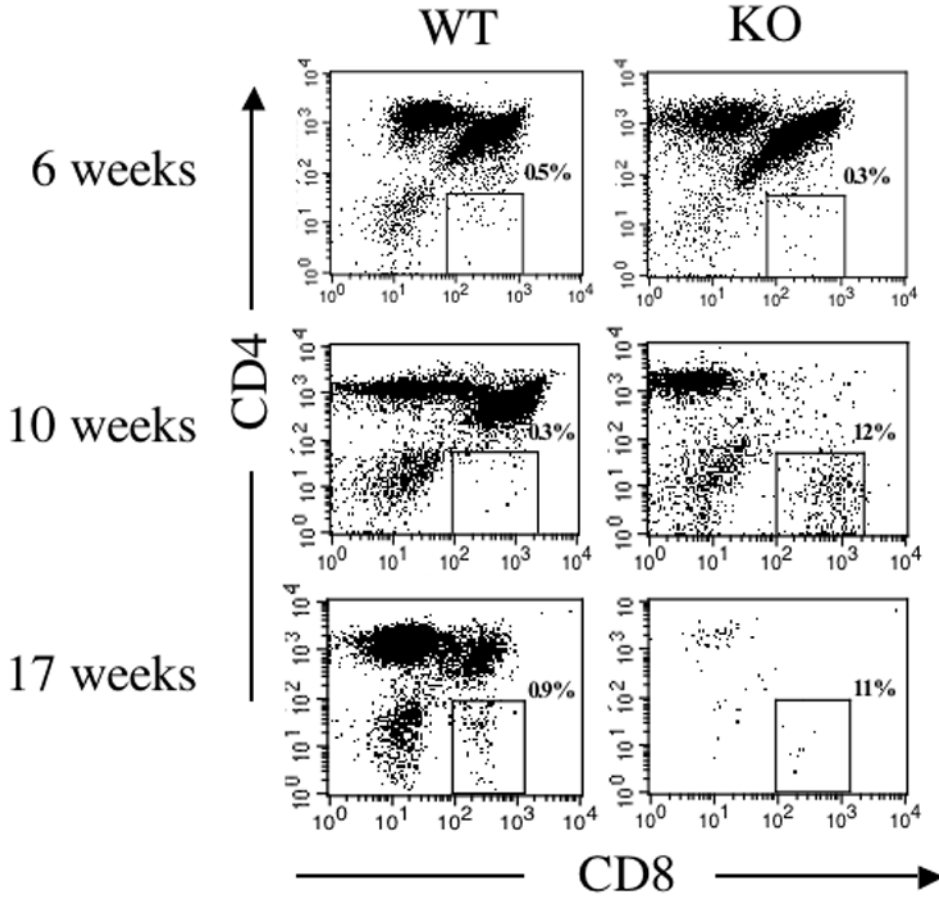


Figure 7. Generation of CD8⁺KJ1-26⁺ T cells in thymuses of RAG-1^{-/-} mice reconstituted with either DO11.10/IL-2 WT or DO11.10/IL-2 KO bone marrow. Thymocytes, prepared from chimeras 6, 10, and 17 weeks post-transplantation, were assessed by flow cytometry for the presence of CD8⁺KJ1-26⁺ T cells. The dot plots shown represent the distribution of CD4⁺, CD8⁺, and CD4⁺CD8⁺ thymocytes within the KJ1-26⁺ thymocyte population. Data shown are representative of 3 or more experiments, with 3 animals per group.

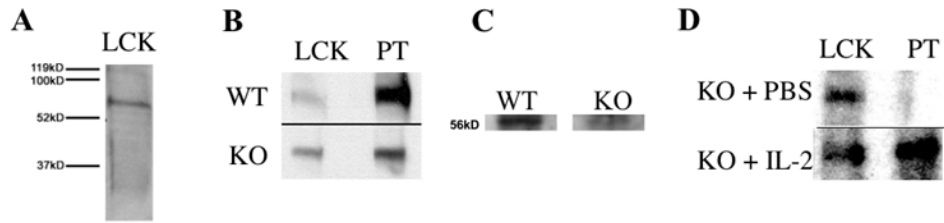


Figure 8.

Activation of thymic lck in severe IL-2 deficiency. (A) Homogenates of whole thymuses were prepared using methods that maintained the phosphorylation state of thymic lck. Western blot analysis of the homogenates with an anti-lck antibody confirmed the presence of 56kD thymic lck. (B) Thymuses from RAG-1^{-/-} mice, 12 weeks post-transplantation with either DO11.10/IL-2 WT or DO11.10/IL-2 KO bone marrow, were prepared as described above. Western blot analysis was then performed to assess the phosphorylation state of lck. Data are representative of 3 experiments, and extracts are from a single animal within one experiment. (C) Thymocyte lysates were prepared from 6 week-old DO11.10/IL-2 WT or KO thymuses. Lck was isolated from the lysates by anti-lck antibodies conjugated to agarose beads, and the phosphorylation state of lck was analyzed by Western blot. Densitometric analysis, performed with NIH Image software, revealed that the band generated from DO11.10/IL-2 WT mice was approximately 2.5 fold darker than that generated from DO11.10/IL-2 KO mice. Data are representative of 3 experiments, and extracts are from a single animal within one experiment. (D) DO11.10/IL-2 KO mice 10 – 15 weeks of age were treated with either PBS or 2 doses of IL-2 (1µg/dose intraperitoneally, 24 h apart) and sacrificed 12 h later. Proteins were extracted and analyzed by Western blot as in A and B. Data are representative of 2 experiments, and extracts are from a single animal within one experiment.